*Journal of Alloys and Compounds, 203* (1994) 281–288
*JALCOM 905*



# Optimization and calculation of the Fe–Ta phase diagram

S. Srikanth* and A. Petric
*Department of Materials Science and Engineering, McMaster University, Hamilton, Ont. (Canada)*

(Received April 19, 1993; in final form July 15, 1993)

**Abstract**

An optimized set of thermodynamic functions was derived for the Fe–Ta system from limited experimental information on phase equilibria and thermodynamics available in the literature using the conjugate gradient method. The thermodynamic properties of the $\epsilon$-phase were described using the sublattice model. For the $\mu$-phase, the enthalpy of formation was estimated from Miedema's model. A Redlich–Kister equation was used to describe the excess thermodynamic functions of the liquid, body-centred cubic and face-centred cubic phases. The phase diagram of the Fe–Ta system was calculated from the evaluated thermodynamic data.

## 1. Introduction

Small additions of tantalum to alloy steels is known to increase the strength of the alloy due to precipitation of tantalum carbide. A knowledge of the phase relationship and thermodynamics of Fe–Ta alloys is essential for the design of these alloys. Information on the enthalpy and Gibbs energy of formation of the Laves phase $Fe_2Ta$ and the $\mu$-phase $Fe_7Ta_6$ are important to the development of structural intermetallic compounds and to analyse the factors contributing to the stability of these intermetallics.

The Laves phase is considered to be stabilized predominantly by the size factor whereas the Frank–Kaspar $\mu$-phase is stabilized by electronic effects rather than size factor effect. Both the $\epsilon$- and $\mu$-phases have some structural similarities and the formation of these phases is governed by the space-filling principle.

Consistency of the thermodynamic data with the phase diagram and vice versa is a good check on the reliability of the measurements. There are very few experimental studies on the Fe–Ta system. The existing experimental information on thermodynamics and phase equilibria is restricted to the Fe-rich portion of the Fe–Ta system. The phase diagram in the regions where little or no experimental information exists can be generated from evaluated thermodynamic data fairly accurately. Further, the advent of powerful computational techniques now enable the calculation of phase diagrams for ternary and multicomponent systems from thermodynamic data. Such calculations require assessed thermodynamic parameters for lower order systems which can be stored in databases. Therefore it is useful to generate a consistent set of thermodynamic parameters for the binary Fe–Ta system valid over the entire range of concentrations.

Phase relationships in iron-rich alloys (0–20 at.% Ta) of the Fe–Ta system are well established. At $X_{Ta} > 0.20$, there are very few experimental measurements at high temperature and the phase diagram is uncertain. This system has been reviewed by Kubaschewski [1] and more recently by Swartzendruber and Paul [2]. The phase diagram at the Fe-rich end is of the contracted $\gamma$-field type and entails two intermediate phases, $\epsilon$, an $MgZn_2$-type Laves phase and $\mu$, with $Fe_7W_6$ structure, both showing significant non-stoichiometry. At the Ta end, there exists a region of solid solubility estimated to extend to 7 at.% Fe.

Optimization and thermodynamic calculation of part of the Fe–Ta phase diagram has been reported earlier by Swartzendruber and Paul [2]. They assumed the intermediate phases $\epsilon$ and $\mu$ to be stoichiometric. The phase diagram calculated from their optimized parameters is in reasonable agreement with experimental data only at low tantalum concentrations. Beyond $X_{Ta} > 0.06$, the liquidus calculated from their evaluated data lies considerably above the experimental values. Further, their evaluated activities in liquid alloys and the Gibbs energy of formation of the $\epsilon$-phase are not in good agreement with later experimental data [3]. At 1873 K, their evaluation leads to a positive deviation from Raoult's law for the activity of iron below $X_{Ta} < 0.4$.

*On leave from National Metallurgical Laboratory, Jamshedpur–831007, India.


*SSDI* 0925-8388(93)00905-E

The vapour pressure measurements of Ichise and Horikawa [3] at 1873 K suggest negative deviation from ideal behaviour for these compositions.

Therefore, we have recalculated the complete phase diagram of the Fe–Ta system in better agreement with the available thermodynamic data. A least squares method using a modified conjugate gradient method has been employed for simultaneously optimizing the experimental data on phase equilibria and thermodynamics.

## 2. Literature data

### 2.1. Phase diagram

The Fe–Ta system has been assessed recently by Swartzendruber and Paul [2]. Their assessed phase diagram is based predominantly on experimental data up to $X_{Ta} = 0.12$. Between $0.12 < X_{Ta} < 0.64$, the liquidus of their assessed diagram appears to be speculative. At the Ta-end, their assessed liquidus, solidus and solvus are based exclusively on thermodynamic calculation. Their proposed diagram is shown in Fig. 1. The experimental information on phase equilibria reported in the literature is briefly reviewed.

Phase equilibria in iron-rich alloys (0–12 at.% Ta) were analysed in the temperature range 1173–1823 K by Sinha and Hume-Rothery [4]. They used thermal analysis to determine the liquidus, the eutectic point ($1713 \pm 2$ K, $X_{Ta} = 0.079$), the eutectoid temperature (1512 K), the peritectoid temperature (1245 K), and employed metallography and dilatometry techniques for the phase boundaries at lower temperatures. Ichise and Horikawa [3] also determined the eutectic invariant temperature to be 1714 ($\pm 2$) K by ion intensity thermal analysis. Fischer *et al.* [5] investigated the Fe-rich region in the temperature interval 1173–1673 K employing magnetic susceptibility measurements. They found the eutectoid (1488 K) as well as the peritectoid (1238 K) to be somewhat lower than that reported by Sinha and Hume-Rothery [4] and Genders and Harrison [6]. Fischer *et al.* [5] reported the width of the $(\gamma + \delta)$ two-phase field to be 0.86–1.38 at.% Ta at 1488 K and that of $(\gamma + \alpha)$ to be 0.4–0.71 at.% Ta at 1238 K. The maximum solid solubility of Ta in ($\alpha$Fe) at 1238 K reported by Fischer *et al.* [5] is somewhat higher than would be expected by an extrapolation of the solubility data, determined through lattice parameter measurements (873–1173 K) by Abrahamson and Lopata [7].

Phase relationships beyond $X_{Ta} > 0.20$ are uncertain. Raman [8] investigated the constitution of alloys in the composition range 20–90 at.% Ta at 1573 K by X-ray analysis and supplemented by metallographic examinations. He confirmed the existence of the Laves phase, $\epsilon$, having a homogeneity range of 28–36 at.% Ta at 1573 K. The congruent melting temperature of the $\epsilon$-phase has been reported to be $\approx 2048$ K by Elliott and Rostocker [9]. Raman [8] also estimated the homogeneity range of the $\mu$-phase to be 49–54 at.% Ta at 1573 K and suggests that this phase melts congruently

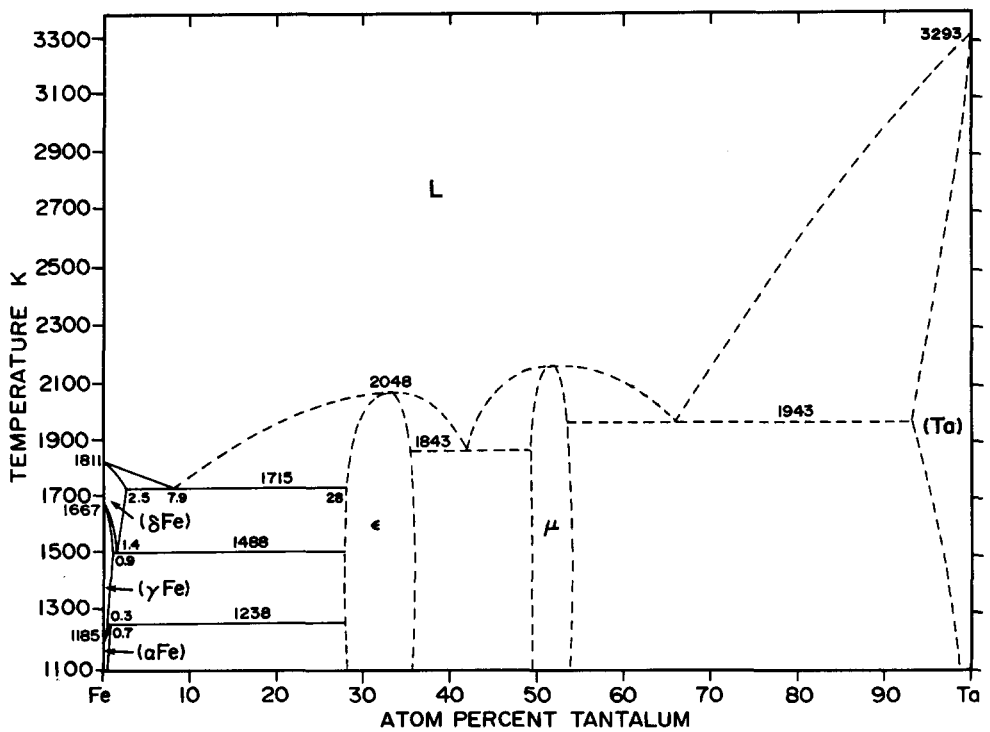


Fig. 1. The phase diagram of the Fe–Ta system proposed by Swartzendruber and Paul.

at a temperature between 2073 and 2173 K. On the contrary, Burlakov and Kogan [10] propose that the $\mu$-phase is formed peritectically at about 1673 K. The melting point of the $\mu$-phase has not been experimentally measured. The peritectic formation of the $\mu$-phase has also been contested by Wetzig [11]. Based on electron microscopy studies, he has proposed that mixtures of the $\epsilon$- and $\mu$-phases decompose eutectically somewhere between 1803 and 1843 K.

Ichise and Horikawa [3] also analysed the constitution of the phases at 1873 K for alloys of $X_{Ta} < 0.64$ by microscopy, electron probe microanalysis (EPMA) and X-ray diffraction of quenched samples. Their results indicate a liquid phase up to 16.8 at.% Ta, the $\epsilon$-phase between 29.4–40.5 at.% Ta, the $\mu$-phase between 49–51 at.% Ta, a two-phase mixture of $(\epsilon+\mu)$ between 40.5 and 49 at.% Ta and a two-phase mixture of $(L+\mu)$ at $X_{Ta}=0.64$. Their findings are in agreement with the previous investigations except for the homogeneity range of the $\epsilon$-phase which appears to be an overestimate. Their results also indicate that the eutectic between the $\epsilon$- and $\mu$-phase possibly occurs at a higher temperature than the 1843 K suggested by Wetzig [11]. The Ta-rich portion of the phase diagram is also uncertain. Raman [8] predicted a eutectic composition close to 63 at.% Ta and estimated the maximum solubility of Fe in (Ta) to be as much as 7 at.%.

### 2.2. Thermodynamic data

#### 2.2.1. Liquid phase

Only two measurements have been reported in the literature on liquid Fe–Ta alloys. Iguchi *et al.* [12] have measured the enthalpy of mixing in liquid alloys containing 2.5–15 at.% Ta at 1866 K. Their results with respect to the pure liquid components standard state is shown in Fig. 2. The activity of iron in Fe–Ta alloys at 1873 K has been measured by Ichise and Horikawa [3] by Knudsen cell mass spectrometry. Their reported partial Gibbs energy of mixing of iron in Fe-rich liquid alloys at 1873 K is shown in Fig. 3.

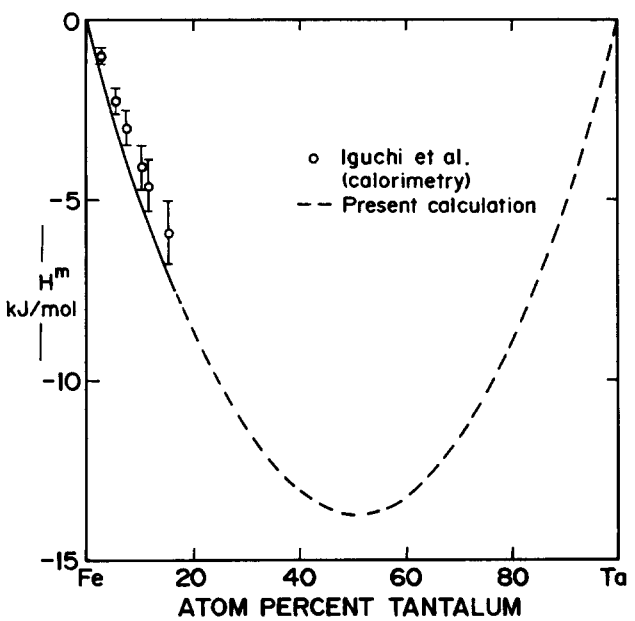


Fig. 2. Calculated enthalpy of mixing in liquid Fe–Ta alloys at 1866 K compared with experimental data (liquid Fe and Ta standard states).

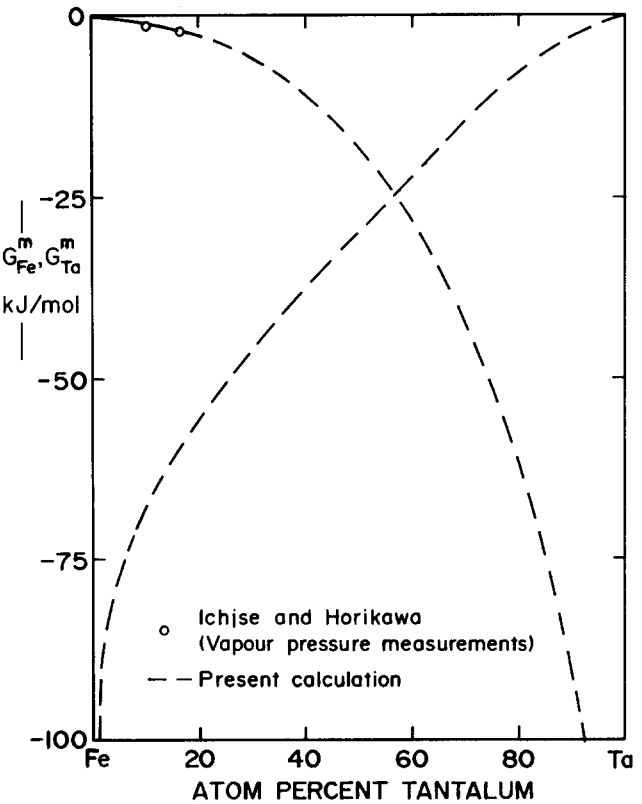


Fig. 3. Calculated partial Gibbs energy of mixing in liquid Fe–Ta alloys at 1873 K compared with experimental results (liquid Fe and Ta standard states).

#### 2.2.2. Solid Phases

Hawkins [13] used an electrochemical cell to determine the activity of Ta along the $\gamma/\gamma+\epsilon$ boundary and found a small positive deviation from ideality. The Gibbs energy of formation of Fe-saturated $\epsilon$-phase was measured by Barby [14] as a function of temperature in the range 1070–1300 K. He employed a non-stationary polarized solid-state galvanic cell using $(LaO_{1.5})ThO_2$ for this purpose. Although he reports the results for the stoichiometry $Fe_2Ta$, the e.m.f. readings correspond to a composition saturated with Fe (*i.e.* $X_{Ta}=0.28$). The Gibbs energy of formation of Fe-saturated $\epsilon$-phase after incorporating corrections for this composition, is given in Table 1. No experimental data exists on the enthalpy or Gibbs energy of formation of the $\mu$-phase.

TABLE 1. Calculated and experimental Gibbs energy of formation of Fe-saturated $\epsilon$-phase [Reference States: f.c.c. Fe and b.c.c. Ta] $\Delta G_f^\circ$ (J g at.$^{-1}$)

| Barby (Experimental) | Swartzendruber and Paul (Evaluation) | Present evaluation |
|---|---|---|
| $-17816+1.243\ T$ | $-12282+0.100\ T$ | $-14785-0.1\ T$ |

## 3. Thermodynamic models

Pure solid elements in their stable form at 298.15 K were chosen as reference for the system. The SGTE (Scientific Group Thermodata Europe) phase stability equations published by Dinsdale [15] were used as the thermodynamic functions of the pure elements. The equations are given in the form of

$$G_i^\circ(T)-H_i^{ser}(298.15\text{K}) = a+bT+cT\ln(T)+dT^2+eT^3+fT^{-1}+gT^n \quad (1)$$

where the stability of the phase is described with respect to the stable element reference (SER) at 298.15K. The parameters used are listed in Table 2. A separate magnetic term described in detail by Hillert and Jarl [16] was included for the body-centred cubic (b.c.c.) Fe phase.

The concentration dependence of the excess Gibbs energy of mixing in the liquid as well as the b.c.c. {($\delta$Fe), ($\alpha$Fe) and (Ta)} solid-solution phases are described by the Redlich–Kister equation:

$$G^E = X_{Ta}(1-X_{Ta})\sum_{\nu=0}^{n}(A_\nu - B_\nu T)(1-2X_{Ta})^\nu \quad (2)$$

The effect of alloying additions on the magnetic Gibbs energy ($G_{mag}{}^m$) of the Fe-rich b.c.c. phase is approximated by a regular solution type behaviour [16]:

$$G_{mag}{}^m = X_{Ta}(1-X_{Ta})^\circ S_{Fe}{}^{mag}\frac{dT_{c(alloy)}}{dX_{Ta}} \quad (3)$$

where $^\circ S_{Fe}{}^{mag}$ is the magnetic entropy of pure b.c.c iron and $T_{c(alloy)}$ is the Curie temperature of the alloy. The Curie temperature was assumed to vary linearly with composition ($T_c = 1043\ X_{Fe}$).

The $\epsilon$-phase is described by a two-sublattice model, $(Fe, Ta)_p(Fe, Ta)_q$, the iron and tantalum atoms can substitute for each other on both sublattices. The Gibbs energy of formation of this phase is represented as:

TABLE 2. Selected values of thermodynamic properties $[G_i(T)-H_i^{ser}]$ of pure elements (from Dinsdale [15])

| Element | Temperature (K) | Phase | Formula |
|---|---|---|---|
| Fe | 298.15–1811 | b.c.c. | $1225.7+124.134T-23.5143T\ln(T)$ $-0.00439752T^2-5.89269\text{E}-8T^3+77358.5T^{-1}+G_{mag}$ |
| | 1811–6000 | b.c.c. | $-25383.581+299.31255T-46.0T\ln(T)$ $+2.29603005\text{E}31T^{-9}+G_{mag}$ |
| | 298.15–1811 | f.c.c. | $-236.7+132.416T-24.6643T\ln(T)$ $-0.00375752T^2-5.89269\text{E}-8T^3+77358.5T^{-1}$ |
| | 1811–6000 | f.c.c. | $-27097.396+300.25256T-46.0T\ln(T)$ $+2.78854\text{E}31T^{-9}$ |
| | 298.15–1811 | Liquid | $13265.87+117.57557T-23.5143T\ln(T)$ $-0.0043975T^2-5.89269\text{E}-8T^3+77358.5T^{-1}$ $-3.6751551\text{E}-21T^7$ |
| | 1811–6000 | Liquid | $-10838.83+291.302T-46.0T\ln(T)$ |
| Ta | 298.15–1300 | b.c.c. | $-7285.889+119.139857T-23.7592624T\ln(T)$ $-2.623033\text{E}-3T^2+0.170109\text{E}-6T^3-3293T^{-1}$ |
| | 1300–2500 | b.c.c. | $-22389.955+243.88676T-41.137088T\ln(T)$ $+6.167572\text{E}-3T^2-0.655136\text{E}-6T^3+2429586T^{-1}$ |
| | 2500–3290 | b.c.c. | $+229382.886-722.59722T+78.5244752T\ln(T)$ $-17.983376\text{E}-3T^2+0.195033\text{E}-6T^3-93813648T^{-1}$ |
| | 298.15–1000 | Liquid | $21875.086+111.561128T-23.7592624T\ln(T)$ $-2.623033\text{E}-3T^2+0.170109\text{E}-6T^3-3293T^{-1}$ |
| | 1000–3290 | Liquid | $43884.339-61.981795T+0.0279523T\ln(T)$ $-12.330066\text{E}-3T^2+0.614599\text{E}-6T^3-352338T^{-1}$ |

$$\Delta G_f(\epsilon) = RT[n_{Fe}^1 \ln(n_{Fe}^1) + n_{Ta}^1 \ln(n_{Ta}^1) + n_{Fe}^2 \ln(n_{Fe}^2) + n_{Ta}^2 \ln(n_{Ta}^2) - N^1 \ln(N^1) - N^2 \ln(N^2)] + \Delta G^* + n_{Ta}^1 G_{Ta}^1 + n_{Fe}^2 G_{Fe}^2 + n_{Fe}^1 n_{Ta}^1 G_0^1 + n_{Fe}^2 n_{Ta}^2 G_0^2 \quad (4)$$

$$X_{Fe} = n_{Fe}^1 + n_{Fe}^2$$
$$X_{Ta} = n_{Ta}^1 + n_{Ta}^2$$
$$N^1 = n_{Fe}^1 + n_{Ta}^1$$
$$N^2 = n_{Fe}^2 + n_{Ta}^2$$

where $n_{Fe}^1$, $n_{Ta}^1$, $n_{Fe}^2$ and $n_{Ta}^2$ are mole fractions of Fe and Ta atoms on sublattices 1 and 2 and $N^1$ and $N^2$ are the site fractions of sublattices 1 and 2. The term $\Delta G^*$ is the Gibbs energy of formation of the perfectly ordered phase at the stoichiometric composition per mole of atoms, $G_{Fe}^2$ and $G_{Ta}^1$ are the Gibbs energy of formation of 1 mol. substitutional Fe or Ta atoms on sublattice 2 and 1, respectively. The parameters $G_0^1$ and $G_0^2$ are coefficients of polynomial interactions between atoms on the same sublattice. The $G$ parameters can assume a temperature dependence of the form

$$G_j^i = A - BT \quad (5)$$

The quantities $n_{Fe}^1$, $n_{Fe}^2$, $n_{Ta}^1$ and $n_{Ta}^2$ are calculated by minimizing the Gibbs energy for a given $X_{Ta}$.

As a result of the absence of any data on the liquid compositions coexisting with the $\mu$-phase, this phase was treated as a stoichiometric compound ($X_{Ta} = 0.52$). The Gibbs energy of formation of the stoichiometric compound is given by the expression

$$\Delta G_f = A - BT \quad (6)$$

The enthalpy of formation of this compound (the constant $A$ in eqn. (6)) was estimated from Miedema's model [17–19]. The model parameters used for the present estimation of the enthalpy of formation of the $\mu$-phase is from Niessen *et al.* [19]. The parameters of Miedema's model are not adjustable in the optimization program.

## 4. The evaluation procedure

The coefficients used for the thermodynamic description of the various phases can be derived by simultaneously optimizing the available thermodynamic and phase equilibrium data. An object function ($S$) is defined as the sum of squared deviations from the experimental values for all the sets of data ($j$):

$$S = \sum_{j=1}^{q_k} N_j \sum_{i=1}^{q_{jk}} W_{ij}(F_{ij} - F_{ij}')^2_i \quad (7)$$

where $W_{ij}$ is the weighting factor for each data point $i$ in the data set $j$ and is related to the uncertainty associated with the experiment, and $N_j$ is a normalization factor. The terms $F_{ij}$ and $F_{ij}'$ are the measured and calculated functions respectively. The upper limits of summation $q_{jk}$ and $q_k$ are the number of data points in the data set $k$ and the number of data sets respectively. The object function is then minimized to give the best values of the model parameters. The minimization is accomplished by the conjugate gradient method introduced by Powell [20]. This method is iterative in nature and does not involve the evaluation of derivatives. Details of this method are available in the original paper of Powell and in an earlier paper on the Fe–Nb system [21]. A coded computer program for Powell's algorithm is given by Brent [22].

The phase diagram can be calculated from the optimized thermodynamic functions by equating the chemical potential of both the components in the coexisting phases with reference to the same standard state. For computing the tie-line compositions involving equilibrium between partially stoichiometric compounds, the procedure proposed by Lukas *et al.* [23] has been used. The resultant set of non-linear equations were solved using a numerical procedure.

## 5. Optimization and calculation of the Fe–Ta system

The thermodynamic data used in the present evaluation are the calorimetric measurements of Iguchi *et al.* [12] and the vapour pressure measurements of Ichise and Horikawa [3] for the Fe-rich liquid phase, the e.m.f. results of Barby [14] and the activity data of ref. 3 at 1873 K for the $\epsilon$-phase and the SGTE pure element data from Dinsdale [15], as given in Table 2. For experimental information on phase equilibria, the thermal analysis results of Sinha and Hume-Rothery [4], the susceptibility measurements of Fischer *et al.* [5] and the solubility measurements of Abrahamson and Lopata [7] have been used in the present optimization and are shown in Fig. 4.

The evaluation commenced with optimizing the parameters of the liquid and b.c.c. phases simultaneously to the thermodynamic data on liquid alloys, Gibbs energy of formation of the Fe-saturated $\epsilon$-phase and phase diagram data at the Fe-rich terminal region. A two-term Redlich–Kister equation was employed for the thermodynamic description of the liquid phase as well as the b.c.c. phase.

In the next step, the $\epsilon$-phase was treated by the sublattice model. The $\epsilon$-phase has a C14 structure isotypic with $Zn_2Mg$ containing 12 atoms per unit cell [24]. There are three atomic positions, two for Fe containing 8 atoms and one for Ta containing 4 atoms.

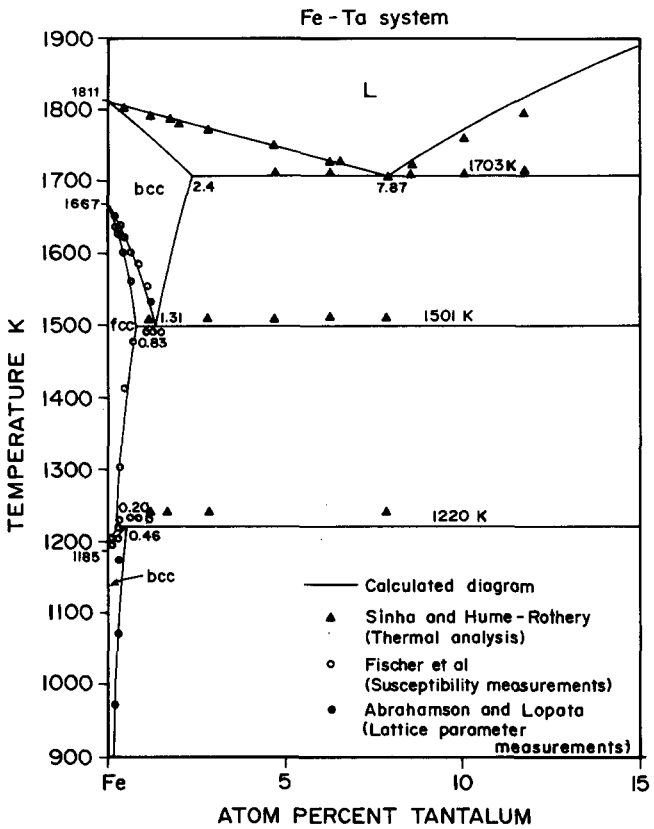


Fig. 4. Calculated and experimental Fe-rich part of the Fe–Ta phase diagram.

Denham [25] has suggested that the non-stoichiometry in $Fe_2Nb$ is a result of substitutional disorder. We assumed this to be valid for the $Fe_2Ta$ phase also whereby the deviation from stoichiometry is a result of disorder due to the presence of Fe atoms on Ta sites and of Ta atoms on Fe sites. Substitution of both elements on both sublattices was assumed allowing the phase to exist over the entire composition range. Keeping the evaluated parameters of the liquid phase constant and using the available tie-line compositions between liquid and $\epsilon$-phase, and the thermodynamic data at the Fe-saturated end, the model parameters for the $\epsilon$-phase were evaluated using the optimization procedure.

For the $\mu$-phase, since experimental information is not available on phase equilibria, the Gibbs energy of formation of this phase cannot be derived from the optimization procedure. Therefore, the enthalpy of formation of this phase was estimated from Miedema's semi-empirical model which is known to be successful for alloys involving a transition metal. Further, it was observed that the calculated enthalpy of formation of the $\epsilon$-phase using Miedema's model was in good agreement with the experimental data of Barby [14]. The entropy of formation of the $\mu$-phase was calculated from the estimated enthalpy of formation and the activity data of Ichise and Horikawa [3] at 1873 K.

## 6. Results and discussion

The evaluated thermodynamic functions for the various phases are given in Table 3. The evaluated enthalpy of mixing of liquid Fe–Ta alloys with reference to pure liquid components standard state is depicted in Fig. 2 along with the calorimetric results of Iguchi *et al.* [12] for comparison. The partial Gibbs energy of mixing with reference to liquid components derived from the present evaluation is shown in Fig. 3 in comparison with the vapour pressure measurements of Ichise and Horikawa [3] on liquid alloys. It is seen from Figs. 2 and 3 that the evaluated thermodynamic functions are in good agreement within the limits of uncertainty with the available experimental data. The Gibbs energy of formation of Fe-saturated $\epsilon$-phase from face-centred

TABLE 3. The evaluated parameters of the Fe–Ta system

| Phase | Model | Parameter | $A$ (J g at.$^{-1}$) | B (J g at.$^{-1}$ K$^{-1}$) | Reference state |
|---|---|---|---|---|---|
| Liquid | Redlich–Kister (2-term) | $X_{Ta}X_{Fe}$ | −54797.3 | −0.9862 | Liquid Fe and Ta |
| | | $X_{Ta}X_{Fe}(1-2X_{Ta})$ | 1118.4 | −12.3462 | |
| b.c.c. | Redlich–Kister (2-term) | $X_{Ta}X_{Fe}$ | 7745.1 | 1.6257 | b.c.c. Fe and b.c.c. Ta |
| | | $X_{Ta}X_{Fe}(1-2X_{Ta})$ | −1847.5 | 1.4478 | |
| f.c.c. | Redlich–Kister (1-term) | $X_{Ta}X_{Fe}$ | 21103.2 | 9.47183 | f.c.c Fe and b.c.c. Ta |
| $\epsilon$-phase | Sublattice model | $\Delta G^*$ | −13697.5 | −3.9488 | f.c.c. Fe and b.c.c. Ta |
| | | $G^2_{Fe}$ | 93793.4 | 11.1537 | |
| | | $G^1_{Ta}$ | 78316.6 | −12.7851 | |
| | | $G^1_0$ | −250231.4 | −11.7029 | |
| | | $G^2_0$ | −264434.6 | 39.4997 | |
| $\mu$-phase | Miedema model and activity data | $\Delta^f G$ | −22000 | −1.3098 | b.c.c. Fe and b.c.c. Ta |

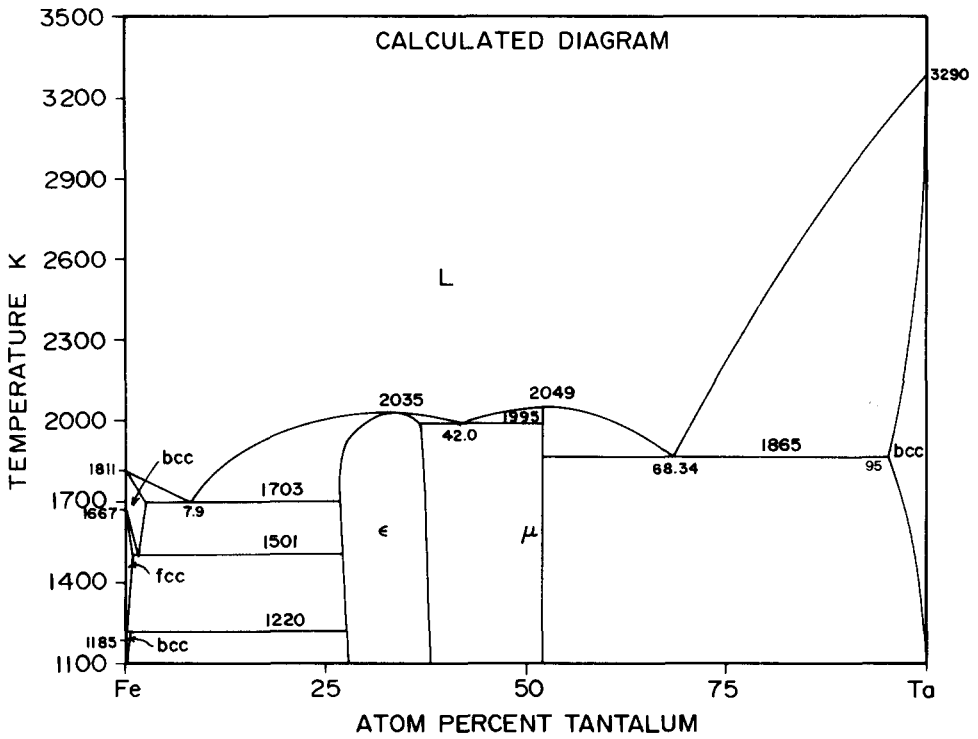


Fig. 5. The calculated Fe–Ta phase diagram.

cubic (f.c.c.) Fe and b.c.c. Ta calculated from the model parameters is shown in Table 1 in comparison with experimental data and the evaluated data of Swartzendruber and Paul [2]. The calculated values are in reasonable agreement with the e.m.f. results of Barby [14].

The detailed Fe-rich portion of the phase diagram calculated from the evaluated thermodynamic functions is shown in Fig. 4 and the complete phase diagram is shown in Fig. 5. The general agreement between the calculated and experimental diagram is very good at the Fe-end where the diagram is fairly well established. The calculated eutectic between the $\epsilon$- and $\mu$-phases (1995 K) agrees with the observation of a two-phase region ($\epsilon+\mu$) at 1873 K by Ichise and Horikawa [3] but is higher than the value of 1843 K suggested by Swartzendruber and Paul [2]. The calculated congruent melting point of the $\mu$-phase (2049 K) is in agreement with that suggested by Raman [8] ($\approx$2073 K). The calculated eutectic at the Ta end and the maximum solubility of Fe in (Ta) is in fair agreement with the proposed values of Raman [8].

## 7. Summary

The Fe–Ta binary system has been evaluated by a least squares minimization procedure employing the conjugate gradient method for the simultaneous optimization of thermodynamic and phase equilibrium data. For the thermodynamic description of the liquid and terminal phases, a Redlich–Kister formalism was used. The intermediate phases were treated by the sublattice model. The experimental data on the Fe–Ta system is well reproduced. The phase diagram of the Fe–Ta system has been constructed by thermodynamic modelling. The calculated diagram is in good agreement with the existing experimental data.

## Acknowledgments

This work has been funded by the Natural Sciences and Engineering Research Council of Canada and by the US Air Force Engineering Foundation Grant RI-3-91-03.

## References

1 O. Kubaschewski, *Iron Binary Phase Diagrams*, Springer-Verlag, New York, 1982, p. 143.
2 L.J. Swartzendruber and E. Paul, *Bull. Alloy Phase Diagrams*, 7 (1986) 254.
3 E. Ichise and K. Horikawa, *ISIJ Int.*, *29* (1989) 843.
4 A.K. Sinha and W. Hume-Rothery, *J. Iron Steel Inst.*, *205* (1967) 671.
5 W.A. Fischer, K. Lorenz, H. Fabritius and D. Schlegel, *Arch. Eisenhuttenwes.*, *41* (1970) 489.
6 R. Genders and R. Harrison, *J. Iron Steel Inst.*, *134* (1936) 173.

7 E.P. Abrahamson and S.L. Lopata, *Trans. AIME, 236* (1966) 76.
8 A. Raman, *Trans. Indian Inst. Metals, 19* (1966) 202.
9 R.P. Elliott and W. Rostocker, *Trans. ASM, 50* (1958) 617.
10 V.D. Burlakov and V.S. Kogan, *Phys. Met. Metallogr., 7* (1959) 67.
11 K. Wetzig, *Phys. Stat. Solidi, 27* (1968) K7.
12 Y. Iguchi, S. Nosomi, K. Saito and T. Fuwa, *Tetsu-to-Hagane, 68* (1982) 633.
13 R.J. Hawkins, *Proc. Int. Symp. Chem. Metall. Iron Steel, University of Sheffield, July, 1971,* Iron and Steel Institute, London, 1973, p. 310.
14 G.B. Barby, *J. Less-Common Met., 22* (1970) 487.
15 A.T. Dinsdale, *CALPHAD, 15* (1991) 317.
16 M. Hillert and M. Jarl, *CALPHAD, 2* (1978) 227.
17 A.R. Miedema, F.R. deBoer, R. Boom and J.F.W. Dorleijn, *CALPHAD, 1* (1976) 341.
18 A.R. Miedema, P.F. deChatel and F.R. deBoer, *Physica, 100* (1980) 1.
19 A.K. Niessen, F.R. deBoer, P.F. deChatel, W.C.M. Mattens and A.R. Miedema, *CALPHAD, 7* (1983) 51.
20 M.J.D. Powell, *Computer J., 7* (1964) 155.
21 S. Srikanth and A. Petric, *Z. Metallkd.,* 1993, in press.
22 R.P. Brent, *Algorithms for Minimization without Derivatives,* Prentice Hall Inc., Englewood Cliffs, New Jersey, 1973.
23 H.L. Lukas, J. Weiss and E.Th. Henig, *CALPHAD, 6* (1982) 229.
24 P. Villars and L.D. Calvert, *Pearson's Handbook of Crystallographic Data for Intermetallic Phases,* ASM, Metals Park, Ohio, 1985.
25 A.W. Denham, *J. Iron Steel Inst., 205* (1967) 435.